STRUCTURAL CONNECTIVITY VIA THE TENSOR-BASED MORPHOMETRY

Seung-Goo Kim[1] *Moo K. Chung*[1,2,3,⋆] *Jamie L. Hanson*[3,4] *Brian B. Avants*[5]
James C. Gee[5] *Richard J. Davidson*[3,4] *Seth D. Pollak*[3,4]

[1]Department of Brain and Cognitive Sciences, Seoul National University, Korea.
[2]Department of Biostatistics and Medical Informatics,
[3]Waisman Laboratory for Brain Imaging and Behavior,
[4]Department of Psychology, University of Wisconsin, Madison, WI, USA.
[5]Penn Image Computing and Science Laboratory, Department of Radiology,
University of Pennsylvania, Philadelphia, PA, USA.

ABSTRACT

The tensor-based morphometry (TBM) has been widely used in characterizing tissue volume difference between populations at voxel level. We present a novel computational framework for investigating the white matter connectivity using TBM. Unlike other diffusion tensor imaging (DTI) based white matter connectivity studies, we do not use DTI but only T1-weighted magnetic resonance imaging (MRI). To construct brain network graphs, we have developed a new data-driven approach called the ϵ-neighbor method that does not need any predetermined parcellation. The proposed pipeline is applied in detecting the topological alteration of the white matter connectivity in maltreated children who have been post-institutionalized in orphanages in East Europe and China.

Index Terms— tensor-based morphometry, structural connectivity, brain network, maltreatment, Jacobian determinant

1. INTRODUCTION

The human brain exhibits one of the most complex networks. This anatomical substrate supports the emergence of the coherent physiological activities in the distant brain regions that make up a functional network [1]. Unlike extensively studied functional brain networks, structural connectivity is not often explored till the introduction of diffusion tensor imaging (DTI). Nowadays, DTI is often used to investigate the structure of axonal fibers in human brains in vivo.

Recently, there has been an attempt of using cross-correlation of cortical thickness as a way to investigate cortical connectivity [2, 3]. Besides the cortical thickness, it is possible to correlate other vowelwise morphometric measures in building whole brain connectivity maps. For instance, we can correlate the Jacobian determinant obtained from the tensor-based morphometry (TBM) framework. The Jacobian determinant measures the change in the volume of a voxel in deforming the template brain to match an individual brain [4]. By correlating the Jacobian determinant at different voxels, we can quantify how the volume change in one voxel is correlated to the volume changes in other voxels. In this sense, correlating Jacobian determinant can be directly used in constructing the whole brain map of corresponding structural changes.

In this paper, we propose to construct a structural connectivity map based on the cross-correlation of the Jacobian determinant for the first time. The main advantage of the proposed technique is that it does not require DTI but still able to construct the population specific connectivity maps only using T1-weighted MRI. Since MRI has been extensively collected than DTI so far in clinical applications, it would be highly beneficial if we can exploit the massive database of MRI collected through the world in the last decade.

The second advantage of the proposed method is that it can build connectivity maps over the whole brain. Cortical thickness based connectivity maps are restricted to the gray matter only. However, neural development such as myelination, axonal growth and glial proliferation contributes the volume of the white matter so it is crucial to look at connectivity maps over the white matter as well [5]. Our approach can build the connectivity maps of the whole brain including the white matter enabling such an investigation.

The proposed framework is applied to the brain networks of the children who have experienced deprivation or neglect in the early stages of life and have been institutionalized in orphanages in East Europe and China but are now living with adopted families in the USA (Post-Institutionalized; PI). It is known that individuals who experience such an early adversity are at heightened risk for a various mental and physical problems. Hanson et al. found smaller local volume in the orbitofrontal cortex, which is known as the central region to emotion and social regulation, in the PI than the age matching normal controls (NC) [6]. Rodent models show that the cytoarchitectural changes in the frontal cortex such as shortening of dendrite length and the reduction of spine density occur by the chronic stress [7]. Thus we expect decreased white matter connectivity in the PIs in the regions including the frontal cortex.

2. METHODS

2.1. Subjects and MRI image

T1-weighted MRIs were collected using a 3T GE SIGNA scanner for 32 PI and 33 NC subjects. Two groups are matched in terms of age and gender but the mean whole brain volume is greater in the PIs than in the NCs (1,808.2 $\pm$ 117.6 cm^3 and 1,690.0 $\pm$ 156.4 cm^3; T(63)= 3.44; $p < 0.001$). These variables are factored out as nuisance covariates in computing partial correlation. Details on the subjects and the image preprocessing pipelines are explained in [6].

The correspondence should be sent to M.K.C (mkchung@wisc.edu). This work was supported by National Institutes of Health Research Grants MH61285 and MH68858 to S.D.P., funded by the National Institute of Mental Health and the Childrens Bureau of the Administration on Children, Youth and Families as part of the Child Neglect Research Consortium, as well as National Institute of Mental Health Grant MH84051 to R.J.D. WCU Grant from the government of Korea to M.K.C. is also acknowledged.

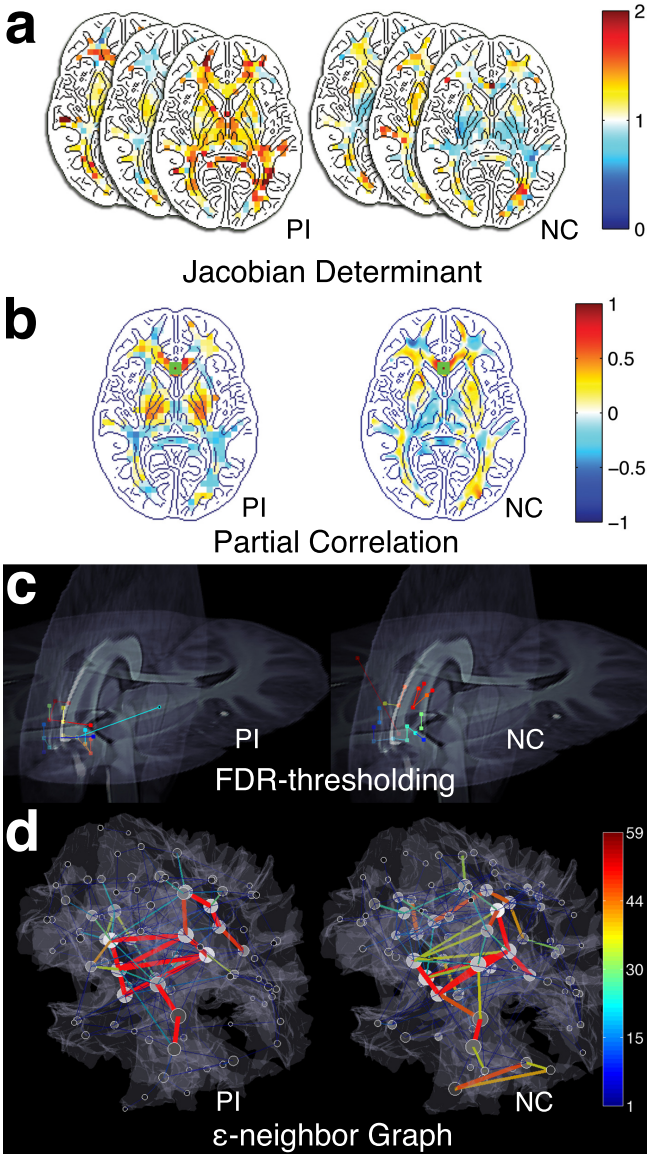

Fig. 1. Framework of the proposed analysis applied to post-institutionalized (PI) children and normal control (NC). **(a)** Jacobian determinant maps of individuals projected on the template. **(b)** partial correlation maps seeded at the genu (marked with green squares) **(c)** FDR-thresholding on partial correlation is used to establish edges of the connectivity network. Only edges connecting near the genu are visualized. The different pairings are marked with different colors. **(d)** The proposed ϵ-neighbor graphs of connectivity. Only positive correlations are shown here. The gray shading of nodes indicates the node degree. The size of nodes represents the number of nodes that are merged in the ϵ-neighbor construction.

The running time for computing the whole correlation matrix quadratically increases as the number of its nodes increases. Even with about 300000 white matter voxels in the template, there are total 90000000000 cross-correlations to compute. The 1mm-resolution Jacobian determinant maps are spatially smoothed out with a Gaussian kernel with 3mm FWHM. This has the effect of representing the Jacobian determinant as the weighted average of neighboring Jacobian determinant. To reduce the computational burden, the Jacobian determinant map are subsampled at every 5mm. Subsequently 2692 nodes are obtained over the white matter (reduction ratio= 0.80 %). This is more than sufficient number of nodes for modeling white matter connectivity and substantially larger than most of connectivity studies that use between 50-100 nodes.

2.2. Partial correlation maps

Fig. 1 illustrates the proposed pipeline. Between 2692 nodes, we link two nodes if the partial correlation of the Jacobian determinants is statistically significant at a certain threshold. The Jacobian determinant is defined as the determinant of the displacement gradient matrix $\partial \mathbf{U}/\partial \mathbf{x}$ [4] as

$$J = \det(I + \partial \mathbf{U}/\partial \mathbf{x}) \tag{1}$$

where $\mathbf{U}$ is the displacement matrix and $\mathbf{x}$ is the coordinate vector.

To remove the possible confounding effect of age, gender and brain size, we used the partial correlation obtained from fitting general linear models (GLM). Let $\mathbf{z}$ = (1, age, gender, volume) be the nuisance covariate vector consisting of age, gender and volume of a subject. Then we modeled the Jacobian determinant on the i-th node as

$$J_i = \mathbf{z}\lambda_i + \epsilon_i \tag{2}$$

where $\lambda_i = (\lambda_{i1}, \ldots, \lambda_{i4})'$ is the unknown parameter vector and ϵ_i is the correlated zero mean Gaussian noise. The residual of the fit is given by $r_i = J_i - \mathbf{z}\widehat{\lambda}_i$, where $\widehat{\lambda}_i$ are the least-squares estimation. It can be shown that the partial correlation ρ_{ij} between J_i and J_j while factoring out the effect of the nuisance covariates $\mathbf{z}$ is simply given by the Pearson correlation between the residuals r_i and r_j [8]. The partial correlation ρ_{ij} is then estimated using the sample correlation as

$$\widehat{\rho}_{ij} = \frac{\sum r_i r_j - \frac{\sum r_i \sum r_j}{n}}{(r_i{}^2 - \frac{(\sum r_i)^2}{n})(r_j{}^2 - \frac{(\sum r_j)^2}{n})} \tag{3}$$

where n is the number of subjects in each group.

2.3. FDR thresholding of partial correlations

In order to obtain the deterministic network graph, we have thresholded the correlated partial correlations using the false discovery rate (FDR) thresholding. The distribution of correlations can be easily approximated using the Fisher transform:

$$z_{ij} = \frac{\tanh^{-1}(\widehat{\rho}_{ij})}{\sqrt{1/(n-3)}} \sim N(0,1). \tag{4}$$

The null hypothesis H_0 is that there is no link between the nodes i and j, i.e. $\rho_{ij} = 0$.

The family-wise error rate (FWER) based thresholding would highly inflated the statistical significance with $2692 \times 2691/2$ possible tests between all nodes. Thus we applied the FDR with $q = 0.01$

under a weak assumption of dependency. If the resulting FDR-threshold is given by s, the adjacency matrix $A = (a_{ij})$ is given by $a_{ij} = 1$ if $z_{ij} \geq s$ and $a_{ij} = 0$ otherwise, with the diagonal terms $a_{ii} = 0$.

2.4. ϵ-neighbor graph simplicaton

Though the obtained adjacency matrices via the FDR thresholding are sparse, almost ten thousands edges still encumber biological interpretation. Furthermore, isolated single connections consisting of two nodes are more likely false positives. Therefore, we need to perform a network simplification without distorting underlying network topology. For this purpose, we have adapted the ϵ-neighbor scheme [9], which was originally applied in constructing network graphs out of numerous white matter tracts obtained from DTI. The algorithm condenses a given complex graph to a much simpler graph iteratively.

From the FDR-thresholding, we obtain collection of significant edges $\mathtt{e}_{i1}\mathtt{e}_{i2}$ linking two nodes $\mathtt{e}_{i1}$ and $\mathtt{e}_{i2}$. Suppose we have constructed the graph $\mathcal{G}_{k-1}$ using edges $\mathtt{e}_{11}\mathtt{e}_{12}, \cdots, \mathtt{e}_{k-1,1}\mathtt{e}_{k-1,2}$ only. Then at the k-th iteration, we construct the graph $\mathcal{G}_k$ using $\mathtt{e}_{k1}\mathtt{e}_{k2}$ somehow. In order to do this, we need to define the ϵ-neighbor of a graph. Let us define the distance $\mathbf{d}(\mathtt{p}, \mathcal{G}_k)$ of a node $\mathtt{p}$ to the graph $\mathcal{G}_k$ as

$$\mathbf{d}(\mathtt{p}, \mathcal{G}_k) = \min_{\mathtt{q} \in \mathcal{V}_k} \|\mathtt{p} - \mathtt{q}\|. \tag{5}$$

If $\mathbf{d}(\mathtt{p}, \mathcal{G}_k) \leq \epsilon$ for some radius ϵ, the node $\mathtt{p}$ is called the ϵ-neighbor of $\mathcal{G}_k$.

Initially the graph $\mathcal{G}_1 = \{\mathcal{V}_1, \mathcal{E}_1\}$ starts with two nodes $\mathcal{V}_1 = \{\mathtt{e}_{11}, \mathtt{e}_{12}\}$ and a single edge $\mathcal{E}_1 = \{\mathtt{e}_{11}\mathtt{e}_{12}\}$. At the 2nd iteration, we check if the new nodes $\mathtt{e}_{21}$ and $\mathtt{e}_{22}$ are the ϵ-neighbor of $\mathcal{G}_1$. We will merge a new node to the existing node in $\mathcal{V}_1$ if the new node is the ϵ neighbor of a node in $\mathcal{V}_1$. The idea is best illustrated with a toy example given in Fig. 2.

Suppose $\mathtt{e}_{21}$ is the ϵ-neighbor of $\mathcal{G}_1$. We assume that $\mathtt{e}_{12}$ is the closet node to $\mathtt{e}_{21}$. Then we merge $\mathtt{e}_{21}$ to $\mathtt{e}_{12}$ and update the vertex and edge sets as $\mathcal{V}_2 = \{\mathtt{e}_{11}, \mathtt{e}_{12}, \mathtt{e}_{22}\}$, $\mathcal{E}_2 = \{\mathtt{e}_{11}\mathtt{e}_{12}, \mathtt{e}_{12}\mathtt{e}_{22}\}$. Other possible scenarios are given in [9]. This merging and deletion process is iteratively performed. However, the original ϵ-neighbor construction method as presented in [9] does not produce a unique graph and it depends on the initial choice of edge set $\mathcal{E}_1$. To guarantee the stability, we decided to update the coordinates of the pre-existing node when a merging occurs. In the toy example, the coordinates of $\mathtt{e}_{12}$ are updated to $\mathtt{e}_{12}{}'$as

$$\mathtt{e}_{12}{}' \leftarrow \frac{\mathtt{e}_{12} n_{12}^1 + \mathtt{e}_{21}}{n_{12}^1 + 1} \tag{6}$$

where n_{ij}^k is the total number of nodes that are merged to the existing node $\mathtt{e}_{ij}$ at the k-th iteration. If the merging happens, we have to update n_{ij}^k as well. So we have $n_{12}^2 = n_{12}^1 + 1$. For this study, ϵ was set to be 21 mm to investigate the connectivity at macro-scale level.

3. RESULTS

The FRD-thresholding produces the connectivity graph with 2692 nodes. The ϵ-neighbor method simplifies the graph with only 88 nodes and 241 edges for the PIs, and 86 nodes and 276 edges for the NCs. In terms of the number of nodes, the ϵ-neighbor method achieves the compression rate of 3.27 % while still preserving the overall topological structures of graph with 2692 nodes.

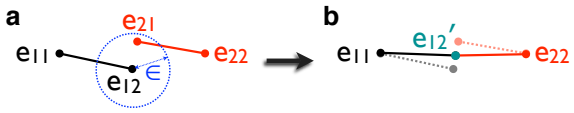

Fig. 2. Schematic illustration of the ϵ-neighbor updating scheme. **(a)** Initially the graph $\mathcal{G}_1$ consists of one edge $\mathtt{e}_{11}\mathtt{e}_{12}$ (black). At the next stage, we determine how to connect the new edge $\mathtt{e}_{21}\mathtt{e}_{22}$ (red) to the existing graph $\mathcal{G}_1$. The node $\mathtt{e}_{21}$ is within the ϵ radius (blue) of the node $\mathtt{e}_{12}$. So $\mathtt{e}_{21}$ is the ϵ-neighbor of $\mathcal{G}_1$ and has to be merged with $\mathtt{e}_{12}$. **(b)** The coordinates of the merged node $\mathtt{e}_{12}$ is updated to $\mathtt{e}_{12}{}'$ (green) and the new edge $\mathtt{e}_{12}{}'\mathtt{e}_{22}$ is included in $\mathcal{G}_2$.

We have used the degree of nodes as a discriminating feature between the two groups. The degree distributions of ϵ-neighbor graphs are shown in Fig. 3. The counts in the high degrees are prone to noise thus those exceeding degree 14 are summed into a single bin [1]. Since the underlying distribution of degree differences is unknown, the significance of the degree differences between groups is tested using a permutation test. We randomly permuted the group identifiers for 2,000 times and proceeded with the graph construction procedures. Since we need to perform multiple tests for 15 degrees simultaneously, the Bonferroni correction threshold for an individual test was set at $0.05/15 = 0.0033$. There are significantly more nodes with the low degrees (1, 3 and 4) in the PIs than the NCs. On the other hand, there are more nodes with the high degrees (7 and 12) in the NCs than the PIs. Since the numbers of nodes are expected to be similar across groups, it suggests that the nodes with the high degrees are affected in the PIs resulting more low degree nodes. It also implicates weakened connectivity in the PIs in accordance with the previous literatures [7].

The anatomical patterns of the ϵ-neighbor graphs are shown in Fig. 4. While the inter-hemispherical edges connecting homologous sub-cortical regions are commonly found in the both groups, the differences in the edge concentration are observed in the regions that include the cerebellar and the brainstem and also in the regions around the anterior cingulate gyri. In addition to the edge concentration, the extension of the edges that reach to the dorsal lateral prefrontal regions and the medial temporal regions seems to be limited in the PIs than in the NCs suggesting consistency with the reduced local volume in those regions [6].

4. DISCUSSIONS

We have presented a novel structural connectivity mapping technique that uses only T1-weighted MRI. The constructed partial correlation maps (Fig.1) look very similar to the probabilistic connectivity maps obtained from DTI. Further research is need for validating the closeness of the partial correlation maps to the probabilistic connectivity maps.

The network graphs showed significantly different degree distributions in PIs implying abnormal connectivity. The anatomical pattern of the white matter connectivity seems to be locally different across groups. However, it should be more thoroughly validated in a further study.

In this paper, we have mainly focused on developing the connectivity mapping technique via the TBM framework and the ϵ-neighbor graph simplification.

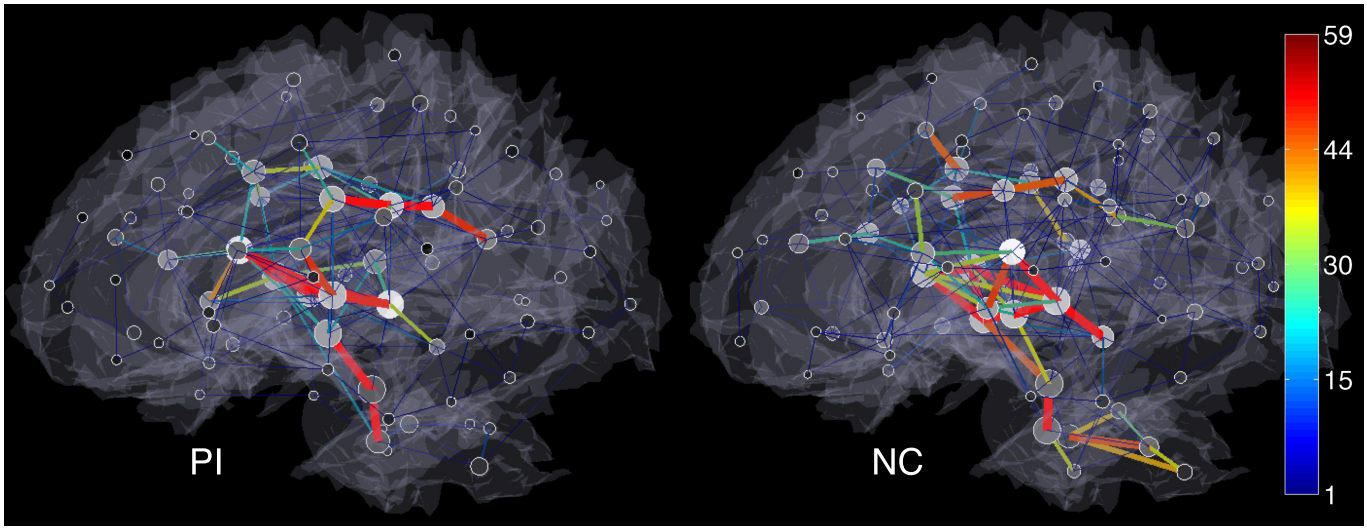

Fig. 4. Local connectivity patterns of the ϵ-neighbor graphs. Only positive correlations are shown in a lateral view. Edges are color-coded by the number of merged connections implying the strength of connections. The gray shading of nodes indicates the degree and the size of nodes represents the number of nodes that are merged.

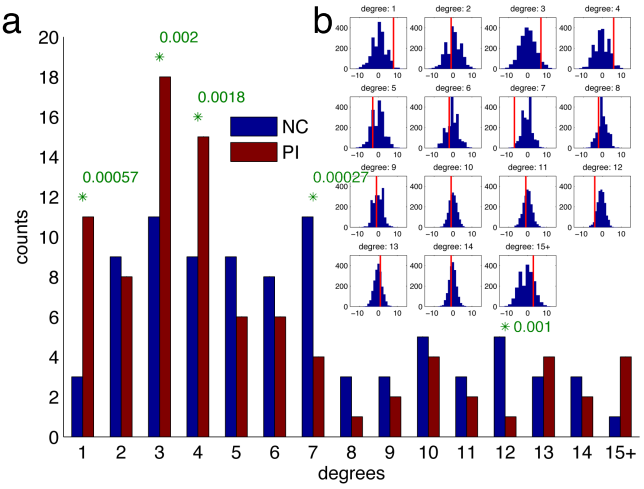

Fig. 3. Permutation tests on degree distributions. **(a)** Degree distributions. The significant differences between the PIs and the NCs marked with green asterisks with p-values (Bonferroni corrected at 0.05). **(b)** The null distribution obtained by 2000 permutation tests. X-axis is for the difference of degrees between the PIs and the NCs. Y-axis is for the number of counts. Red vertical lines note the actual differences.

5. REFERENCES

[1] E. Bullmore and O. Sporns, "Complex brain networks: graph theoretical analysis of structural and functional systems," *Nature Reviews Neuroscience*, vol. 10, no. 3, pp. 186–198, 2009.

[2] J.P. Lerch, K. Worsley, W.P. Shaw, D.K. Greenstein, R.K. Lenroot, J. Giedd, and A.C. Evans, "Mapping anatomical correlations across cerebral cortex (MACACC) using cortical thickness from MRI," *Neuroimage*, vol. 31, no. 3, pp. 993–1003, 2006.

[3] Y. He, Z. Chen, and A. Evans, "Structural insights into aberrant topological patterns of large-scale cortical networks in alzheimer's disease," *Journal of Neuroscience*, vol. 28, no. 18, pp. 4756, 2008.

[4] M.K. Chung, K.J. Worsley, T. Paus, D.L. Cherif, C. Collins, J. Giedd, J.L. Rapoport, , and A.C. Evans, "A unified statistical approach to deformation-based morphometry," *NeuroImage*, vol. 14, pp. 595–606, 2001.

[5] S. Groeschel, B. Vollmer, MD King, and A. Connelly, "Developmental changes in cerebral grey and white matter volume from infancy to adulthood," *International Journal of Developmental Neuroscience*, 2010.

[6] J.L. Hanson, M.K. Chung, B.B. Avants, E.A. Shirtcliff, J.C. Gee, R.J. Davidson, and S.D. Pollak, "Early stress is associated with alterations in the orbitofrontal cortex: A tensor-based morphometry investigation of brain structure and behavioral risk," *Journal of Neuroscience*, vol. 30, no. 22, pp. 7466, 2010.

[7] A. F. T. Arnsten, "Stress signalling pathways that impair prefrontal cortex structure and function," *Nature Reviews Neuroscience*, vol. 10, no. 6, pp. 410–422, 2009.

[8] Eric D. Kolaczyk, *Statistical Analysis of Network Data: Methods and Models*, Springer Publishing Company, Incorporated, 2009.

[9] M.K. Chung, N. Adluru, K.M. Dalton, A.L. Alexander, and R.J Davidson, "Scalable brain network construction on white matter fibers," in *SPIE Medical Imaging*, 2010.